

# Long-term laser frequency stabilization using fiber interferometers

Jia Kong,<sup>1,2, a)</sup> Vito Giovanni Lucivero,<sup>1</sup> Ricardo Jiménez-Martínez,<sup>1</sup> and Morgan W. Mitchell<sup>1,3</sup>

<sup>1)</sup>ICFO – Institut de Ciències Fòniques, Mediterranean Technology Park, 08860 Castelldefels, Barcelona, Spain

<sup>2)</sup>Quantum Institute for Light and Atoms, Department of Physics, State Key Laboratory of Precision Spectroscopy, East China Normal University, Shanghai 200062, China

<sup>3)</sup>ICREA – Institució Catalana de Recerca i Estudis Avançats, 08015 Barcelona, Spain

(Dated: 19 August 2020)

We report long-term laser frequency stabilization using only the target laser and a pair of 5 m fiber interferometers, one as a frequency reference and the second as a sensitive thermometer to stabilize the frequency reference. When used to stabilize a distributed feedback laser at 795 nm, the frequency Allan deviation at 1000 s drops from  $5.6 \times 10^{-8}$  to  $6.9 \times 10^{-10}$ . The performance equals that of an offset lock employing a second, atom-stabilized laser in the temperature control.

## I. INTRODUCTION

Laser linewidth and frequency stability are critical in laser spectroscopy and its many applications. Short-term linewidth can be narrowed by active feedback from a fast frequency discriminator such as an optical cavity<sup>1</sup> or an interferometer<sup>2</sup>, and is limited by the speed of the feedback and the noise of the discriminator signal<sup>3</sup>. Long-term stability above hundreds milliseconds<sup>3,4</sup>, in contrast, requires stabilization to an absolute reference and is limited by slow changes in the reference and in the feedback system. As references, atomic and molecular lines are very stable but give low signal to noise ratios and a limited selection of frequencies<sup>5,6</sup>. For this reason, if long-term stability at a frequency far from atomic and molecular lines is needed, linewidth narrowing is often combined with a transfer lock in which a first laser is stabilized to an atomic or molecular transition, a discriminator is stabilized to this laser, and a second laser is stabilized to the discriminator, possibly at a different wavelength<sup>4</sup>.

The complexity of this approach can in principle be avoided if the frequency discriminator itself provides a stable reference. Here we demonstrate stabilization of a distributed-feedback (DFB) diode laser to two unbalanced Mach-Zehnder interferometers (MZIs), one used to stabilize the temperature of the other, interrogated with the same target laser. The system derives its stability from the material properties of silica fiber and a metal, in our case an aluminum alloy. We observe the same long-term stability as using two independent lasers for MZIs, e.g.  $6.9 \times 10^{-10}$  at 1000 s. Although much less stable than the best optical cavities<sup>3</sup>, our setup provides long-term stability with lower cost and complexity. An application requiring this level of stability is quantum-enhanced magnetometry<sup>7,8</sup>, which will also require many-GHz detunings in the spin-exchange-relaxation-free regime<sup>9,10</sup>.

Unbalanced fiber interferometers have recently

emerged as suitable references to sense and stabilize laser frequency. The interferometer phase  $\phi$  is very sensitive to laser frequency  $f$  due to the large physical path difference  $L$ :

$$\phi = \frac{2\pi n}{c} f L, \quad (1)$$

where  $n$  is the refractive index of the fiber and  $c$  is the speed of light. Prior work includes MZI stabilization of a helium-neon laser to 5 kHz linewidth<sup>2</sup> over a time scale of 1 s, stabilization erbium-doped fiber distributed-feedback lasers (EDFLs)<sup>11–13</sup>, e.g. to 8 Hz linewidth<sup>13</sup> over 1 s using a 2 km path-imbalanced Michelson interferometer (MI). The linewidth of DFB diode lasers<sup>14,15</sup> has shown large narrowing factors, e.g. from 370 kHz to 18 Hz over 1 ms using a MI<sup>14</sup> and from 3 MHz to 15 kHz using a MZI<sup>15</sup>. 50 Hz peak-to-peak non-linearity frequency error was also achieved in an agile laser with high sweep linearity<sup>16</sup>.

Long-term stability has been little studied with unbalanced interferometers and the above works only achieved short-term linewidth reduction with long-term stability affected by temperature fluctuations. For example, in<sup>15</sup> there is no stability improvement over times longer than 64 s. To achieve long-term stability, Chiodo *et al.*<sup>17</sup> used a high-precision electronic temperature controller with well-designed physics package<sup>18</sup> to control the fiber’s temperature. Without high-precision electronics, Wang *et al.*<sup>19</sup> implemented a transfer lock using an atomic reference to control the temperature of a 2 m path-imbalanced Young’s interferometer, and stabilized an external cavity diode laser to  $10^{-8}$  over 10–4000 s.

## II. OPERATING PRINCIPLE

In our scheme, one interferometer, the “frequency control interferometer” (FCI), is used to sense and stabilize the laser frequency, while a second, “temperature control interferometer” (TCI) is used to sense and eliminate fluctuations in the temperature of the thermal reservoir to which both are attached. As both interferometers are

<sup>a)</sup>Corresponding author:jia.kong@icfo.es

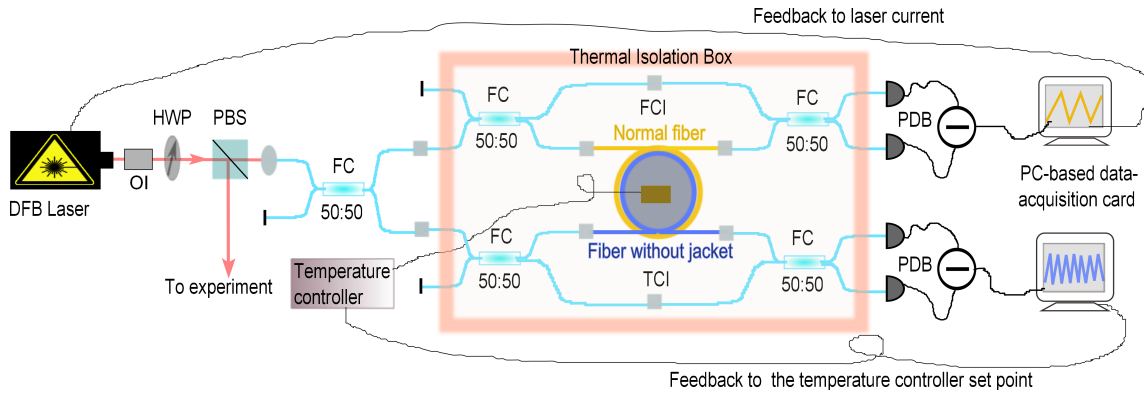


FIG. 1. Schematic of laser frequency locking system. Using a half-wave plate (HWP) and a polarizing beam splitter (PBS), a few 10s of  $\mu\text{W}$  of power from the laser to be stabilized, a DFB (EYP-DFB 795) with wavelength 795 nm followed by an optical isolator (OI), is injected into a fiber system containing two unequal-path Mach-Zehnder interferometers. Each interferometer is composed of two 50:50 fiber couplers (FC) and an additional 5 m fiber to imbalance the paths. In the frequency control interferometer (FCI) the extra fiber is a jacketed single mode fiber, while for the temperature control interferometer (TCI), it is a polarization maintaining fiber without jacket. The fibers are wound around a 10 cm diameter aluminum cylinder fitted with a resistive heater and a resistive temperature sensor. In each interferometer the output powers are collected on a Thorlabs balanced amplified photodetector (PDB450C), providing signals that are used for feedback, either to the laser current, or to the set-point of a temperature controller from Wavelength Electronics (model HTC1500) by a digital controller (PC-based data-acquisition card). The interferometers are enclosed in a insulation layer of extruded polystyrene foam.

interrogated using the same target laser, this scheme provides a simpler alternative to approaches relying on a second reference laser<sup>4,19</sup>. The FCI and TCI are constructed to have the same frequency response

$$\frac{d\phi}{df} = \frac{2\pi nL}{c} = 0.1522 \frac{\text{rad}}{\text{MHz}}, \quad (2)$$

where  $n = 1.454^{20}$  and  $L = 5$  m (equal for the two interferometers). Larger  $L$  would give better frequency discrimination, but a larger device.

The TCI is designed to have a much stronger temperature response than the FCI, which can be achieved by reducing the temperature sensitivity of the latter by using a special fiber<sup>21</sup>. Here we instead increase the temperature sensitivity of the TCI by using a jacketless fiber, tightly wound on an aluminum cylinder, as the extra length in the TCI. The coefficient of thermal expansion (CTE)  $\alpha = L^{-1}dL/dT$  of aluminum,  $\alpha_{\text{Al}} = 23 \times 10^{-6} \text{ K}^{-1}$ , is 40 times larger than the CTE of silica fiber  $\alpha_{\text{SiO}_2} = 0.5 \times 10^{-6} \text{ K}^{-1}$ , while the two materials have very similar Young's moduli, so the fiber is stretched by the aluminum cylinder as the temperature  $T$  rises, giving  $dL_{\text{TCI}}/dT > dL_{\text{FCI}}/dT$ .

In the TCI, phase change with temperature arises from the interaction of the thermo-optic coefficient  $dn/dT$ , the CTE, and the elasto-optic coefficient  $dn/dL$

$$\frac{d\phi_{\text{TCI}}}{dT} = \frac{2\pi L}{\lambda} \frac{dn}{dT} + \frac{d\phi_{\text{TCI}}}{dL_{\text{TCI}}} \frac{dL_{\text{TCI}}}{dT}, \quad (3)$$

where  $\lambda = c/f$ . The first part of Eq. (3) describes the thermo-optic effect, while the second part combines the other two effects. In contrast the FCI is not stretched, so there is no elasto-optic effect and the phase change with

temperature is

$$\frac{d\phi_{\text{FCI}}}{dT} = \frac{2\pi L}{\lambda} \frac{dn}{dT} + \frac{2\pi n}{\lambda} \frac{dL_{\text{FCI}}}{dT}. \quad (4)$$

With  $\lambda = 795$  nm,  $dn/dT = 9.2 \times 10^{-6} \text{ K}^{-1}$ ,  $d\phi_{\text{TCI}}/dL_{\text{TCI}} = 9.14 \times 10^6 \text{ rad/m}^{22}$ ,  $L^{-1}dL_{\text{TCI}}/dT = \alpha_{\text{Al}}$ , and  $L^{-1}dL_{\text{FCI}}/dT = \alpha_{\text{SiO}_2}$  we find  $d\phi_{\text{TCI}}/dT = 1414 \text{ rad/K}$  and  $d\phi_{\text{FCI}}/dT = 392 \text{ rad/K}$  and thus the TCI is 3.6 times more sensitive to temperature than the FCI.

### III. EXPERIMENTAL REALIZATION

The setup is shown and described in FIG. 1. To stabilize the frequency of a DFB laser, we use MZIs with differential detection, which allows rejecting common-mode intensity fluctuations, a two-fold increase in slope because the outputs are anti-phase, and in principle, shot-noise limited performance. In the TCI, the additional 5 m fiber has no jacket but retains a  $60 \mu\text{m}$  acrylate coating applied during manufacture. This fiber is tightly wrapped by hand around the aluminum cylinder while at room temperature. The expansion to reach the 60 degree Celsius operating point exceeds the coating thickness and guarantees the fiber is always under tension. In this case, a polarization maintaining (PM) fiber is used to prevent stress-induced polarization fluctuation. The 5 m fiber of the FCI, which has a  $328 \mu\text{m}$  jacket, is wrapped on the same aluminum cylinder. This guarantees good thermal contact of the two fibers with a single thermal reservoir, but the FCI does not stretch significantly.

FIG. 2 shows the two interferometer's responses to frequency and temperature scans. As there is a mi-

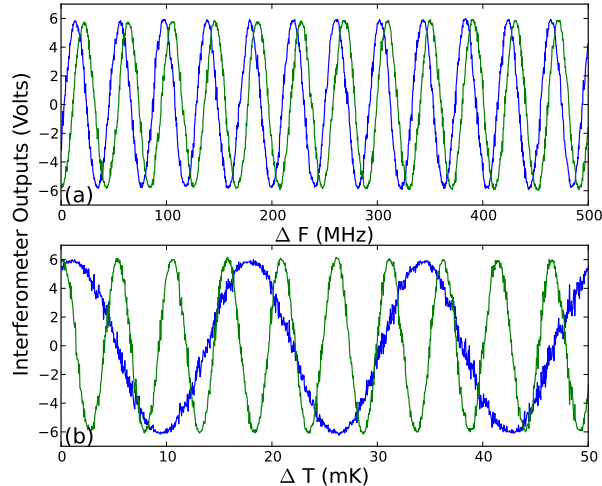


FIG. 2. Interferometers' phase response to temperature and frequency. (a) Differential outputs of the FCI (blue) and TCI (green) as laser frequency is scanned by  $\Delta F$ .

(b) Same signals as interferometers' temperature is scanned by  $\Delta T$ . While the frequency response is matched, the TCI is about three times more sensitive to temperature changes.

nor length difference between FCI and TCI, their responses to frequency are not perfectly matched. This does not strongly affect the stabilization, which maintains a unique frequency/temperature combination provided the interferometers' sensitivity to temperature and to frequency are different. We calibrate the frequency response against a  $^{87}\text{Rb}$  absorption spectrum to find 0.1544 rad/MHz (TCI), 0.1540 rad/MHz (FCI), which are close to the 0.1522 rad/MHz expected from Eq. (2). We calibrate the temperature response against a thermistor and find 1211 rad/K (TCI) and 400 rad/K (FCI), which agree reasonably well with the values found above.

The output of the FCI can be fed back to the laser current to stabilize the laser frequency. The output of the TCI can similarly be fed back to the set point of the temperature controller to stabilize the temperature of the aluminum cylinder. Both controls are realized with a 100 kHz bandwidth data acquisition card. Without the feedback from TCI, the thermal gain (ratio of laboratory fluctuations to system fluctuations) of the system is about 400, and it improves by a factor of 3 when the TCI is used as temperature probe to further stabilize the set point of the temperature controller.

#### IV. RESULTS AND DISCUSSIONS

To monitor the frequency fluctuations of the target laser, we interfered the laser output against a second laser stabilized by saturated absorption spectroscopy to the  $D_1$  line of Rb. This reference laser had a stability, measured by beating against a duplicate laser, of  $\leq 8 \times 10^{-11}$  at

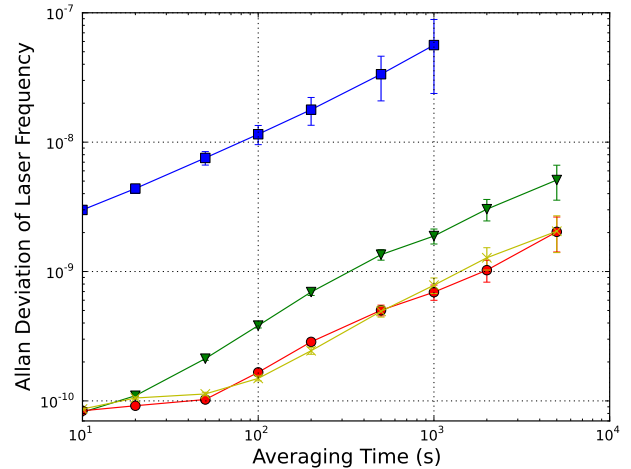


FIG. 3. Allan deviation of DFB laser frequency under various control scenarios. Free running laser (blue squares), frequency stabilization by FCI feedback to laser current (green triangles), temperature stabilization by TCI feedback to temperature controller, in addition to frequency stabilization (red circles), and temperature stabilization by TCI feedback, but with the TCI injected by a separate laser frequency stabilized by saturated-absorption spectroscopy (yellow stars). Error bars are obtained by dividing by the square root of the number of samples in each averaging time interval<sup>24</sup>.

1000 s and a  $t^{1/2}$  scaling, an order of magnitude better than the lasers under test. The resulting beat note was recorded on a spectrum analyzer and the computed centroid of the spectrum was taken as the current frequency. We collected the frequency every 10 seconds over 15 hours of total acquisition, and compute the Allan deviation<sup>23</sup> for various control scenarios, shown and described in FIG. 3.

As expected, stabilization to the FCI provides better stability, by about a factor of 30 for all time scales measured. For times above about 1 minute, the TCI provides a further improvement by about a factor of 2.5 which is larger in longer time scale, giving a relative frequency stability (Allan deviation) of  $8.5 \times 10^{-11}$  at 10 s and  $2.0 \times 10^{-9}$  at 5000 s. Multiplying these numbers by the laser central frequency we find 32 kHz at 10 s and 754 kHz at 5000 s. The long-time scaling is  $t^{1/2}$ , characteristic of a frequency random walk. To show how the different temperature response of the FCI and TCI can help a single laser to distinguish between variations in frequency and in temperature, we used a second laser, stabilized to the saturated absorption spectrum of Rb-85  $D_1$  line as the input to the TCI for temperature stabilization. The resulting Allan deviation is indistinguishable from that observed by self-stabilization of the DFB laser, demonstrating that our measurement is not limited by using the target laser for temperature stabilization. This makes our technique competitive with the transfer lock, while being inexpensive, compact and flexible. Moreover,

with this technique, the laser can be locked far from an atomic or molecular frequency reference by counting the number of interference fringes.

We have concentrated on improving long-term frequency stability, as short-term stabilization with fiber interferometers has been well studied<sup>15</sup>. A single fiber interferometer can provide both short-term and long-term stability, using a fast feedback controller with good long-term stability. Using a 5 m path-imbalanced fiber interferometer and high-bandwidth feedback, they narrowed the linewidth of a DFB laser from 3 MHz to 15 kHz. Combined with our self-referencing method, the laser linewidth can be reduced for both short and long time scales.

Atmospheric pressure, vibration and polarization fluctuations are other factors that can limit this locking performance, so vacuum tank and vibration isolation can be used for further improvement<sup>2,13</sup>. Temperature inhomogeneity may still exist, which could be reduced by interleaving the two fibers on their mutual support.

## V. CONCLUSION

In conclusion, we have described a flexible long-term laser frequency stabilization method using two interferometers with very different temperature coefficients. Using only a single laser, we can lock to frequencies not corresponding to any atomic or molecular line. We observe an Allan deviation of  $6.9 \times 10^{-10}$  at 1000 s, an improvement by a factor of 81 relative to the laser with electronic temperature and current stabilization. The laser stability can achieve  $8.5 \times 10^{-11}$  at 10 s and  $2.0 \times 10^{-9}$  at 5000 s. The method is compatible with short-term linewidth narrowing and with integrated interferometers, promising a small, robust, cheap and flexible DFB laser with both short-term and long-term frequency stability.

## VI. ACKNOWLEDGMENTS

We thank Federica Beduini for technical help and useful discussions, Thomas Vanderbruggen for advice on the data analysis and Joanna Zielińska for the loan of a balanced photodetector. This work was supported by the

Spanish MINECO project MAGO (Ref. FIS2011-23520), European Research Council project AQUOMET and Fundación Privada CELLEX. J. K. is supported by the China Scholarship Council project and the Fostering Project for National Top Hundred Doctoral Dissertations (No. PY2013006).

- <sup>1</sup>R. Drever, J. Hall, F. Kowalski, J. Hough, G. Ford, A. Munley, and H. Ward, *Appl. Phys. B* **31**, 97 (1983).
- <sup>2</sup>Y. T. Chen, *Appl. Opt.* **28**, 2017 (1989).
- <sup>3</sup>T. Kessler, C. Hagemann, C. Grebing, T. Legero, U. Sterr, F. Riehle, M. J. Martin, L. Chen, and J. Ye, *Nat Photonics* **6**, 687 (2012).
- <sup>4</sup>A. Rossi, V. Biancalana, B. Mai, and L. Tomassetti, *Review of Scientific Instruments* **73**, 2544 (2002).
- <sup>5</sup>W. Demtröder, *Laser Spectroscopy*, Advanced texts in physics (Springer, 2003).
- <sup>6</sup>H. Tsuchida, M. Ohtsu, T. Tako, N. Kuramochi, and N. Oura, *Japanese Journal of Applied Physics* **21**, L561 (1982).
- <sup>7</sup>F. Wolfgramm, A. Cerè, F. A. Beduini, A. Predojević, M. Koschorreck, and M. W. Mitchell, *Phys. Rev. Lett.* **105**, 053601 (2010).
- <sup>8</sup>V. G. Lucivero, P. Anielski, W. Gawlik, and M. W. Mitchell, *Review of Scientific Instruments* **85**, 113108 (2014).
- <sup>9</sup>R. Jiménez-Martínez, W. C. Griffith, S. Knappe, J. Kitching, and M. Prouty, *J. Opt. Soc. Am. B* **29**, 3398 (2012).
- <sup>10</sup>R. Jiménez-Martínez, S. Knappe, and J. Kitching, *Review of Scientific Instruments* **85**, 045124 (2014).
- <sup>11</sup>G. A. Cranch, *Opt. Lett.* **27**, 1114 (2002).
- <sup>12</sup>K. Takahashi, M. Ando, and K. Tsubono, *Journal of Physics: Conference Series* **122**, 012016 (2008).
- <sup>13</sup>F. Kéfélian, H. Jiang, P. Lemonde, and G. Santarelli, *Opt. Lett.* **34**, 914 (2009).
- <sup>14</sup>J.-F. Cliche, M. Allard, and M. Têtu, *Proc. SPIE* **6216**, 62160C (2006).
- <sup>15</sup>W.-K. Lee, C. Y. Park, J. Mun, and D.-H. Yu, *Review of Scientific Instruments* **82**, 073105 (2011).
- <sup>16</sup>H. Jiang, F. Kéfélian, P. Lemonde, A. Clairon, and G. Santarelli, *Opt. Express* **18**, 3284 (2010).
- <sup>17</sup>N. Chiodo, K. Djerroud, O. Acef, A. Clairon, and P. Wolf, *Appl. Opt.* **52**, 7342 (2013).
- <sup>18</sup>R. Boudot, C. Rocher, N. Bazin, S. Galliou, and V. Giordano, *Review of Scientific Instruments* **76**, 095110 (2005).
- <sup>19</sup>Z. B. Wang, J. W. Zhang, S. G. Wang, K. Miao, and L. J. Wang, *Appl. Opt.* **53**, 3283 (2014).
- <sup>20</sup>D. B. Leviton and B. J. Frey, *Proc. SPIE* **6273**, 62732K (2006).
- <sup>21</sup>V. Dangui, H. Kim, M. Dignonnet, and G. Kino, *Opt. Express* **13**, 6669 (2005).
- <sup>22</sup>M. Silva-López, A. Fender, W. N. MacPherson, J. S. Barton, J. D. C. Jones, D. Zhao, H. Dobb, D. J. Webb, L. Zhang, and I. Bennion, *Opt. Lett.* **30**, 3129 (2005).
- <sup>23</sup>D. W. Allan, *Proceedings of the IEEE* **54**, 221 (1966).
- <sup>24</sup>D. Howe, D. Allan, and J. Barnes, in *Proc. 35th Annu. Symp. on Freq. Contrl.* (1981) pp. 1–47.